

# LncRNA SNHG1 alleviates myocardial ischaemia–reperfusion injury by regulating the miR-137-3p/KLF4/TRPV1 axis

Ruo-Fu Tang<sup>1,2</sup>, Wen-Jing Li<sup>1</sup>, Yun Lu<sup>1</sup>, Xuan-Xuan Wang<sup>1</sup> and Su-Yu Gao<sup>1\*</sup>

<sup>1</sup>Department of Pharmacy, Zhongnan Hospital of Wuhan University, Wuhan, China; and <sup>2</sup>The Second Affiliated Hospital of Zhejiang University, Hangzhou, 310009, China

## Abstract

**Aims** Myocardial ischaemia–reperfusion injury (MIRI) contributes to serious myocardial injury and even death. Long non-coding RNAs (lncRNAs) have been reported to play pivotal roles in the occurrence and development of MIRI. Here, the detailed molecular mechanism of lncRNA SNHG1 in MIRI was explored.

**Methods and results** A cell model of MIRI was established through hypoxia/reoxygenation (H/R) stimulation. Cell viability and pyroptosis were evaluated utilizing MTT, PI staining, and flow cytometry. Interleukin (IL)-1 $\beta$  and IL-18 secretion levels were examined by ELISA. The gene and protein expression were detected by RT-qPCR and western blot, respectively. Dual luciferase reporter gene, RIP and ChIP assays were performed to analyse the molecular interactions. The results showed that lncRNA SNHG1 overexpression alleviated H/R-induced HL-1 cell pyroptosis (all  $P < 0.05$ ). LncRNA SNHG1 promoted KLF4 expression by sponging miR-137-3p. miR-137-3p silencing alleviated H/R-induced pyroptosis in HL-1 cells (all  $P < 0.05$ ), which was abolished by KLF4 knockdown (all  $P < 0.05$ ). KLF4 activated the AKT pathway by transcriptionally activating TRPV1 in HL-1 cells (all  $P < 0.05$ ). TRPV1 knockdown reversed the alleviation of SNHG1 upregulation on H/R-induced pyroptosis in HL-1 cells (all  $P < 0.05$ ).

**Conclusions** These results showed that lncRNA SNHG1 assuaged cardiomyocyte pyroptosis during MIRI progression by regulating the KLF4/TRPV1/AKT axis through sponging miR-137-3p. Our findings may provide novel therapeutic targets for MIRI.

**Keywords** KLF4; LncRNA SNHG1; MiR-137-3p; Myocardial ischaemia–reperfusion injury; TRPV1

Received: 26 June 2023; Revised: 14 November 2023; Accepted: 18 December 2023

\*Correspondence to: Su-Yu Gao, Department of Pharmacy, Zhongnan Hospital of Wuhan University, No. 169 Donghu Road, Hubei Province, Wuhan 430071, China.

Email: 513368394@qq.com

Ruo-Fu Tang and Wen-Jing Li are co-first authors.

## Introduction

Myocardial ischaemia–reperfusion (MIR) is a terrifically effective treatment for myocardial infarction (MI) within a certain time limit.<sup>1</sup> However, new evidence shows that reperfusion after myocardial ischaemia may induce further myocardium damage and threaten human life.<sup>2</sup> Therefore, it is extremely essential to seek methods for alleviating MIR injury (MIRI). Pyroptosis is a newly discovered programmed cell death process characterized by nod-like receptor protein-3 (NLRP3) inflammasome-mediated caspase-1 activation, which often occurs in various organs and tissues under stressful

conditions.<sup>3</sup> Pyroptosis can also induce immoderate cell inflammatory damage.<sup>4</sup> Notably, pyroptosis activation is a key risk factor for MIRI advancement,<sup>5</sup> and pyroptosis inhibition can markedly inhibit MIRI development.<sup>6</sup> Therefore, pyroptosis inhibition has been proposed as a potential treatment method for MIRI.

Long non-coding RNAs (lncRNAs) are a type of non-coding RNA with more than 200 nucleotides, that play an important role in cardiovascular system function.<sup>7,8</sup> A considerable number of lncRNAs have been discovered to have intimate regulatory connections with MIR.<sup>9–11</sup> For instance, Niu X and colleagues showed that lncRNA Oip5-as1 combined with

miR-29a to assuage MIRI through disinhibiting the SIRT1/AMPK/PGC1 $\alpha$  pathway.<sup>10</sup> LncRNA SNHG1, as an eye-catching lncRNA, has been extensively studied in a variety of diseases, including cancer, cardiac hypertrophy, epilepsy, and MIRI.<sup>12–15</sup> For example, lncRNA SNHG1 expression in human umbilical vein endothelial cells was reduced by H/R treatment, and its overexpression alleviated the injury by cardiac I/R via mediating HIF-1 $\alpha$ /VEGF pathway, indicating that lncRNA SNHG1 play a pivotal role in MIRI.<sup>13</sup> However, the mechanisms of lncRNA SNHG1 in MIRI remain unclear.

MicroRNAs (miRNAs) are endogenous non-coding RNAs with around 22 nucleotides, which sequences can regulate the expression of the target gene at the post-transcriptional level.<sup>16,17</sup> The research of miRNA involves various disease fields, certainly, including MIRI.<sup>18,19</sup> MiR-137-3p has been studied in multiple diseases and play crucial roles in these diseases such as cancers, MIRI, and spinal cord ischaemia-reperfusion.<sup>19–21</sup> As previously described, the expression of miR-137-3p was significantly elevated in MI patients, I/R-injured rat and H/R-injured H9C2 cells, and miR-137-3p silencing obviously repressed H/R-induced cardiomyocyte apoptosis by interacting with KLF15,<sup>19</sup> implying that miR-137-3p served as a risk factor in MIRI. However, the exact molecular processes of miR-137-3p remains unknown.

Transient receptor potential vanilloid 1 (TRPV1) is a member of the vanilloids (TRPV) subfamily which is contained in transient receptor potential (TRP) ion channels. TRPV1 has been demonstrated to play critical roles in the development of MIRI.<sup>22–24</sup> A study indicated that apoptotic cardiomyocytes were substantially greater in the hearts of TRPV1<sup>-/-</sup> mice given I/R than in WT mice given I/R,<sup>22</sup> indicating that TRPV1 may function as a protective factor in MIRI. Furthermore, TRPV1 may modulate the PI3K/AKT signalling pathway to attenuate MIRI.<sup>22</sup>

Kruppel-like factor-4 (KLF4) is a known protective factor in MIRI that can protect cardiomyocytes against myocardial injury, inflammatory response, oxidative stress response, and cardiomyocyte death.<sup>25</sup> Based on the above evidence, it is speculated that lncRNA SNHG1 inhibits cardiomyocyte pyroptosis to alleviate MIRI by regulating the miR-137-3p/KLF4/TRPV1 axis. Our work provides a theoretical basis for developing novel therapeutic strategies for MIRI.

## Methods

### Cell culture and treatment

HL-1 cardiomyocytes were obtained from Sigma Aldrich (Saint Louis, MO, USA). Cells were cultured in Claycomb medium (Sigma Aldrich) supplemented with 10% fetal bovine serum, 1% penicillin, 1% streptomycin, 0.1 mM noradrenaline, and

2 mM L-glutamine under the condition of a humidified chamber with 5% CO<sub>2</sub> and at 37°C.

To construct the hypoxia-reoxygenation (H/R) model, HL-1 cells were cultured in DMEM with 1% O<sub>2</sub>, 94% N<sub>2</sub> and 5% CO<sub>2</sub> for 16 h, followed by reoxygenation for 6 h.<sup>26</sup>

### Cell transfection

Oe-lncRNA SNHG1, miR-137-3p mimics/inhibitor, sh-KLF4, sh-TRPV1 as well as their negative control groups (pcDNA3.1, mimics NC and inhibitor NC, sh-NC) were purchased from GenePharma (Shanghai, China). HL-1 cells (5 × 10<sup>4</sup> cells/well) were cultured in 24-well plates (Corning, NY, USA) and subjected to transfection when reaching to 60% confluency. A total of 0.8  $\mu$ g plasmid (oe-SNHG1 or oe-NC or sh-KLF4 or sh-TRPV1 or sh-NC) was incubated with 50  $\mu$ L serum-free medium (in the case involving co-transfection of multiple plasmids, the amount between plasmids was 1:1), and 0.8  $\mu$ L Lipofectamine™ 3000 was incubated with 50  $\mu$ L serum-free medium for 30 min. Then, serum free medium containing plasmids and Lipofectamine™ 3000 were mixed and left for 20 min at room temperature. The original medium in the plate was discarded, and 400  $\mu$ L serum-free medium and the mixed solution were added to the culture well. After 6 h, it was replaced to complete culture medium, and cells were cultured for 24 h. A total of 0.8  $\mu$ g miRNA (miR-137-3p mimics/inhibitor or mimics/inhibitor NC) was incubated with 50  $\mu$ L serum-free medium, and 0.8  $\mu$ L lipo 3000 was incubated with 50  $\mu$ L serum-free medium for 30 min. Then, serum free medium containing miRNA and lipo 3000 were mixed and left for 20 min at room temperature. The original medium in the plate was discarded, and 400  $\mu$ L serum-free medium and the mixed solution were added to the culture well. After 6 h, it was replaced to complete culture medium, and cells were cultured for 24 h. The transfection protocol figure was shown in *Figure S1*. The sequences of miRNA mimics and shRNAs were listed as follows:

miR-137-3p mimics:

5'-UUUUAUGCUAAGAAUACGCGUAG-3',  
5'-CUACGCGUAUUCUUAAGCAAUA-3'.

Mimics NC:

5'-UCACAACCUCCUAGAAAAGAGUAGA-3',  
5'-UCUACUCUUUCUAGGAGGUUGUGA-3'.

miR-137-3p inhibitor:

5'-CUACGCGUAUUCUUAAGCAAUA-3',

NC inhibitor:

5'-UCUACUCUUUCUAGGAGGUUGUGA-3',

sh-KLF4:

5'-AATTGGCGTGAGGAACTCTCTCACATTCAAGAGA  
atgtgagagagttcctcacgcTTTTT-3',  
5'-GATCAAAAAGCGTGAGGAACTCTCTCACATTCTCTGA  
AatgtgagagagttcctcacgcC-3'.

sh-TRPV1:

5'-AATTGGGAAGACAGATAGCCTGAAGCTTCAAGAG  
AgcttcaggctatctgtcttccTTTTT-3',  
5'-GATCAAAAAGGAAGACAGATAGCCTGAAGCTCTCTGA  
AgcttcaggctatctgtcttccC-3'.

sh-NC:

5'-AATTGTTCTCCGAACGTGTCACGTTTCAAGAGAACGTGACA  
CGTTCGGAGAATTTTTT-3',  
5'-GATCAAAAATTCTCCGAACGTGTCACGTTCTCTTGAAACG  
TGACACGTTCCGGAGAAC-3'.

### 3-(4,5-dimethylthiazol-2-yl)-2,5-diphenyltetrazolium bromide (MTT) assay

HL-1 cell viability was detected using the MTT assay kit (BTN111105, Bjalb, Beijing, China) according to the instruction. In brief, cells were seeded in 96-well plates (200  $\mu$ L,  $3 \times 10^3$  cells per well) and incubated with MTT solution (20  $\mu$ L) for 4 h. Next, 150  $\mu$ L DMSO was applied to dissolve the formazan crystals. A microplate reader (Thermo Fisher Scientific) was employed to evaluate the absorbance at 490 nm after the MTT reaction.

### Western blot

The proteins were isolated with RIPA lysis buffer (Beyotime), and the protein concentration was tested using the BCA protein kit (Beyotime). Following that, total protein (20  $\mu$ g) was separated using 10% SDS-PAGE and transferred to a Millipore PVDF membrane. The membranes were then blocked and incubated with the primary antibodies against KLF4 (abcam, Cambridge, UK, 1:1000, #ab129473), TRPV1 (abcam, 1:1000, #ab203103), NLRP3 (abcam, 1:1000, # ab263899), Cleaved caspase 1 (Cell Signalling Technology, MA, USA, 1:1000, #89332), Cleaved Gasdermin-D (Cell Signalling Technology, 1:1000, #34667), AKT (1:500, # ab8805), p-AKT (1:1000, # ab38449) and  $\beta$ -actin (1:5000, # ab6276) overnight at 4°C. Subsequently, the membranes were incubated with the HRP-conjugated secondary antibody for 1 h. The blots were visualized by the ECL kit (Beyotime) using the Gel imager (Biorad, CA, USA). The densitometry analysis was performed using Image J.

### RNA isolation, reverse transcription, and RT-qPCR

The total RNA was extracted with TRIzol (Invitrogen, Carlsbad, USA). The cDNA was synthesized with the Prime Script Reverse Transcription Reagent Kit (TaKaRa, Shiga, Japan) and subjected to RT-qPCR assay using the SYBR Premix Ex Taq II Kit (Takara, Shiga, Japan). All data were calculated by using  $2^{-\Delta\Delta t}$  method. GAPDH was regarded as reference gene.

### Flow cytometry assay

Cell pyroptosis was detected by the FAM-FLICA *in vitro* Caspase-1 Detection Kit (Immunochemistry Technologies, MN, USA). HL-1 cells were stained with 10  $\mu$ L of FAM-FLICA and 2  $\mu$ g/mL of PI following the manufacturer's protocol. The percentage of Cleaved caspase 1 represented the ratio of cell pyroptosis of HL-1 cells, which was further quantified using flow cytometry (BD Biosciences, NJ, USA).

### Cell death assay

HL-1 cells were cultured on coverslips until the cell confluence reached 80%. Cells were then stained with 6  $\mu$ L of DAPI solution and 6  $\mu$ L of PI (Sangon, Shanghai, China) at 4°C in the dark for 20 min. Cells were subsequently observed under a fluorescence microscope (Olympus, Tokyo, Japan). Cell death was analysed by calculating the proportion of PI positive cells to the total cells in the field of view.

### Enzyme-linked immunosorbent assay (ELISA)

The secretion levels of interleukin (IL)-1 $\beta$  and IL-18 were examined by the mouse IL-1 $\beta$  ELISA kit (Solarbio, Beijing, China, SEKM-002) and the mouse IL-18 ELISA kit (Beyotim, PI553), respectively. All operations were strictly carried out according to the instructions. The data were analysed in the microplate spectrophotometer (Biotek, Beijing, China).

### Dual luciferase reporter gene assay

The sequences of lncRNA SNHG1/KLF4 containing the binding site of miR-137-3p were cloned into psiCHECK2 vectors (Ke Lei Biological Technology Co., Ltd, China) to construct reporter vectors lncRNA SNHG1/KLF4 (WT/MUT). miR-137-3p mimics couple with lncRNA SNHG1/KLF4 (WT/MUT) were transfected into the HL-1 cardiomyocytes by Lipofectamine<sup>™</sup> 3000 (Invitrogen, CA, USA). After 48 h, the luciferase activity was detected using a dual-luciferase reporter assay system (Promega, Madison, USA) abiding by the protocol.

The promoter fragment of TRPV1 was cloned into a pGL3 vector to construct TRPV1-WT or TRPV1-MUT vector. Then, TRPV1-WT/TRPV1-MUT vector and oe-KLF4 were co-transfected into HL-1 cardiomyocytes using Lipofectamine™ 3000. The relative luciferase activity was tested by normalizing the firefly luminescence to the renilla luminescence.

### RNA immunoprecipitation (RIP) assay

RIP was performed using a Magna RIP RNA-Binding Protein Immunoprecipitation kit (Millipore, MA, USA) according to the manufacturer's instruction. Briefly, the cell lysates were incubated with magnetic beads conjugated with negative control normal mouse IgG or human anti-Ago2 antibody (Millipore). The immunoprecipitated RNAs were then extracted and detected by RT-qPCR to confirm the enrichment of binding targets.

### Chromatin immunoprecipitation (ChIP) assay

Cells were fixed with 1% formaldehyde solution for 10 min, quenched with 125 mM glycine for 5 min and fragmented into 200–500 bp length fragments by sonication. The cell lysate was subsequently incubated with anti-KLF4 (Abcam, 1:50, ab214666) or anti-IgG (Abcam, 1:1000, ab171870) at 4°C overnight. Immunoprecipitated DNAs were purified and analysed by gel electrophoresis.

### Statistical analyses

All the data from three independent experiments and expressed as mean  $\pm$  standard deviation (SD). All statistical analyses were calculated using GraphPad Prism (version 8.0). Student's *t*-tests were used to examine the differences between the two groups. To analyse the differences across several groups, one-way ANOVA was used, followed by Tukey's post hoc test. When  $P < 0.05$ , there were significant differences between the data.

## Results

### lncRNA SNHG1 overexpression alleviated H/R-induced pyroptosis in HL-1 cells

As shown in *Figure 1A*, lncRNA SNHG1 expression in HL-1 cells was significantly reduced by H/R treatment. HL-1 cells were transfected with oe-NC or oe-SNHG1, and the results of RT-qPCR showed that oe-SNHG1 transfection significantly elevated SNHG1 expression in HL-1 cells (*Figure S2A*). Functional experiments subsequently showed that SNHG1 overexpres-

sion had no significant effect on HL-1 cell viability (*Figure S2B*) and pyroptosis (*Figure S2C*) under physiological condition. To further investigate the role of SNHG1 in regulating pyroptosis during MIRI progression, SNHG1 overexpression was induced in H/R-treated HL-1 cells. In brief, HL-1 cardiomyocytes were transfected with oe-NC or oe-SNHG1 for 48 h, followed by hypoxia (16 h)-re-oxygenation (6 h). The detailed protocol figure was shown in *Figure 1B*. It was observed that the inhibitory effect of H/R on SNHG1 expression in HL-1 cells was reversed by oe-SNHG1 transfection (*Figure 1C*). In terms of biological functions, lncRNA SNHG1 upregulation prevented H/R-induced decrease in HL-1 cell viability and ameliorated H/R-induced increase in IL-1 $\beta$  and IL-18 secretion, pyroptosis and cell death (*Figure 1D–G*). In addition, we added a cardioprotection control (metoprolol) to compare the effect of the investigated protective pathway as previously reported.<sup>27</sup> HL-1 cells were treated with 5  $\mu$ M metoprolol for 24 h and then exposed to H/R stimulation, and the results showed that both SNHG1 overexpression and metoprolol treatment could alleviate H/R-induced decrease in HL-1 cell viability (*Figure S3*). Meanwhile, western blot results showed that H/R-induced increase in NLRP3, Cleaved caspase 1 and Cleaved Gasdermin-D protein levels in HL-1 cells was ameliorated by SNHG1 overexpression (*Figure 1H*). Collectively, H/R-induced pyroptosis in HL-1 cells was mitigated by SNHG1 overexpression.

### SNHG1 inhibited miR-137-3p expression by directly targeting miR-137-3p

It was observed that miR-137-3p expression in HL-1 cells was significantly increased by H/R treatment (*Figure 2A*). Notably, dual luciferase reporter gene assay results showed that lncRNA SNHG1 directly bound with miR-137-3p (*Figure 2B*), indicating that lncRNA SNHG1 served as a sponge for miR-137-3p. Meanwhile, as revealed by Ago2-RIP assay, SNHG1 directly bound with miR-137-3p (*Figure 2C*). In addition, SNHG1 overexpression ameliorated H/R-induced increase in miR-137-3p expression in HL-1 cells (*Figure 2D*). Taken together, SNHG1 inhibited miR-137-3p expression by sponging miR-137-3p.

### miR-137-3p inhibited KLF4 expression by directly binding to KLF4

As previously described, KLF4 expression was markedly reduced in the myocardial tissue of MIRI rats.<sup>25</sup> Herein, our results showed that KLF4 mRNA and protein levels in HL-1 cells were significantly decreased by H/R stimulation (*Figure 3A,B*). The binding relationship between miR-137-3p and KLF4 was later validated using a dual luciferase reporter gene assay (*Figure 3C*). In addition, miR-137-3p overexpression re-

**Figure 1** lncRNA SNHG1 overexpression alleviated H/R-induced pyroptosis in HL-1 cells. (A) HL-1 cells were subjected to H/R treatment, and SNHG1 expression in cells was detected by RT-qPCR. HL-1 cardiomyocytes were transfected with oe-NC or oe-SNHG1 for 48 h, followed by hypoxia (16 h)-re-oxygenation (6 h), grouping: Control, H/R, H/R + oe-NC and H/R + oe-SNHG1. (B) The detailed protocol figure was presented. (C) SNHG1 expression in cells was assessed using RT-qPCR. (D) Cell viability was assessed using MTT assay. (E) ELISA was adopted to examine IL-1 $\beta$  and IL-18 secretion. (F) Cell pyroptosis was monitored by flow cytometry. (G) Cell death was measured by PI staining. (H) Western blot was employed to determine NLRP3, Cleaved Caspase 1, and Cleaved Gasdermin-D protein levels in HL-1 cells. The measurement data were presented as mean  $\pm$  SD. All data were obtained from three independent repeated experiments. \* $P < 0.05$ , \*\* $P < 0.01$ , \*\*\* $P < 0.001$ .

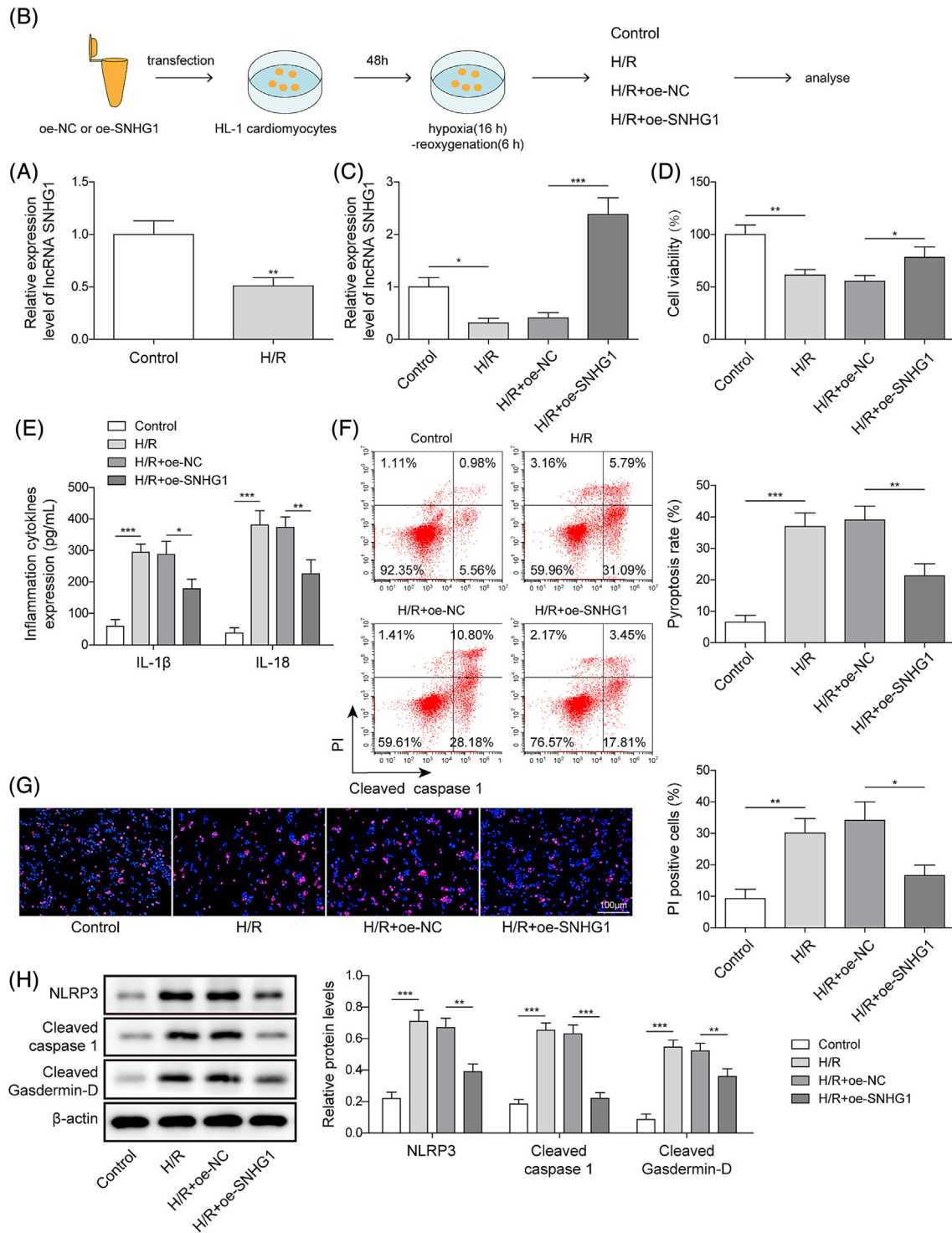
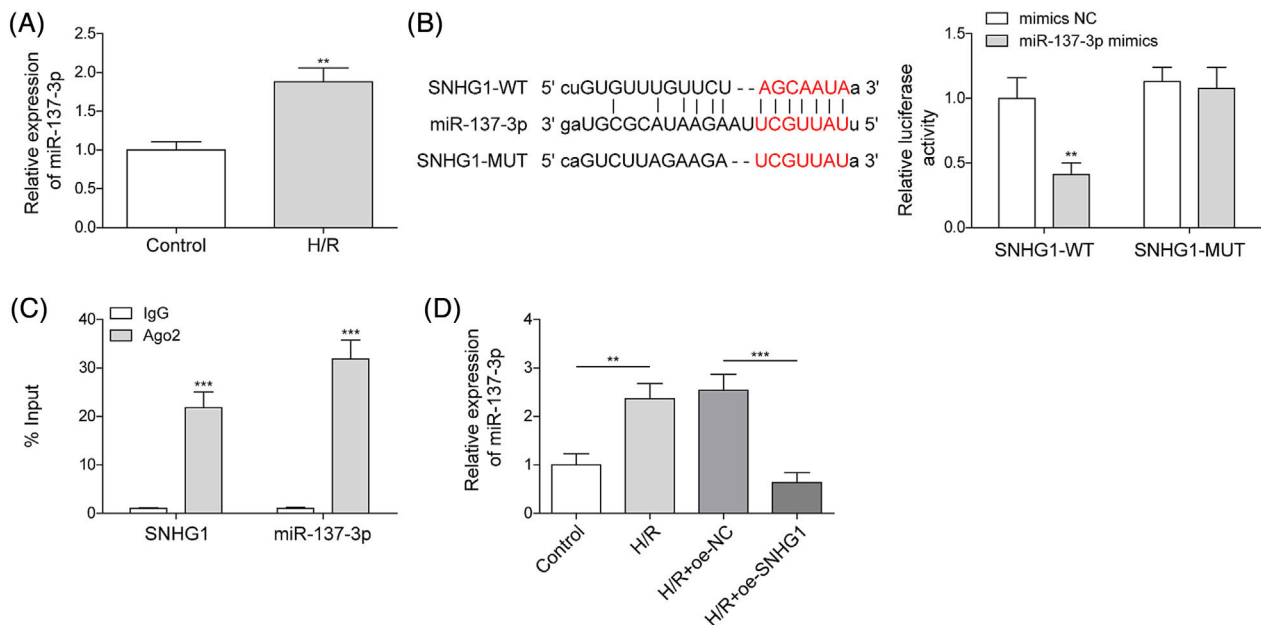




**Figure 2** SNHG1 inhibited miR-137-3p expression by directly targeting miR-137-3p. (A) HL-1 cells were subjected to H/R treatment, and miR-137-3p expression in cells was examined using RT-qPCR. (B) The potential binding site of miR-137-3p on lncRNA SNHG1 was presented, and its interaction was affirmed by dual luciferase reporter gene assay. (C) The interaction between SNHG1 and miR-137-3p was analysed by RIP assay. (D) SNHG1 overexpression was induced in H/R-treated HL-1 cells by transfecting oe-SNHG1 into cells, and miR-137-3p expression in cells was determined by RT-qPCR. The measurement data were presented as mean  $\pm$  SD. All data were obtained from three independent repeated experiments. \* $P < 0.05$ , \*\* $P < 0.01$ , \*\*\* $P < 0.001$ .



duced KLF4 expression level in H/R-treated HL-1 cells, while miR-137-3p inhibition presented the opposite effect (*Figure 3D,E*). All these findings revealed that miR-137-3p decreased KLF4 expression directly in cardiomyocytes during MIRI development.

### miR-137-3p inhibition alleviated H/R-induced pyroptosis in HL-1 cells by increasing KLF4 expression

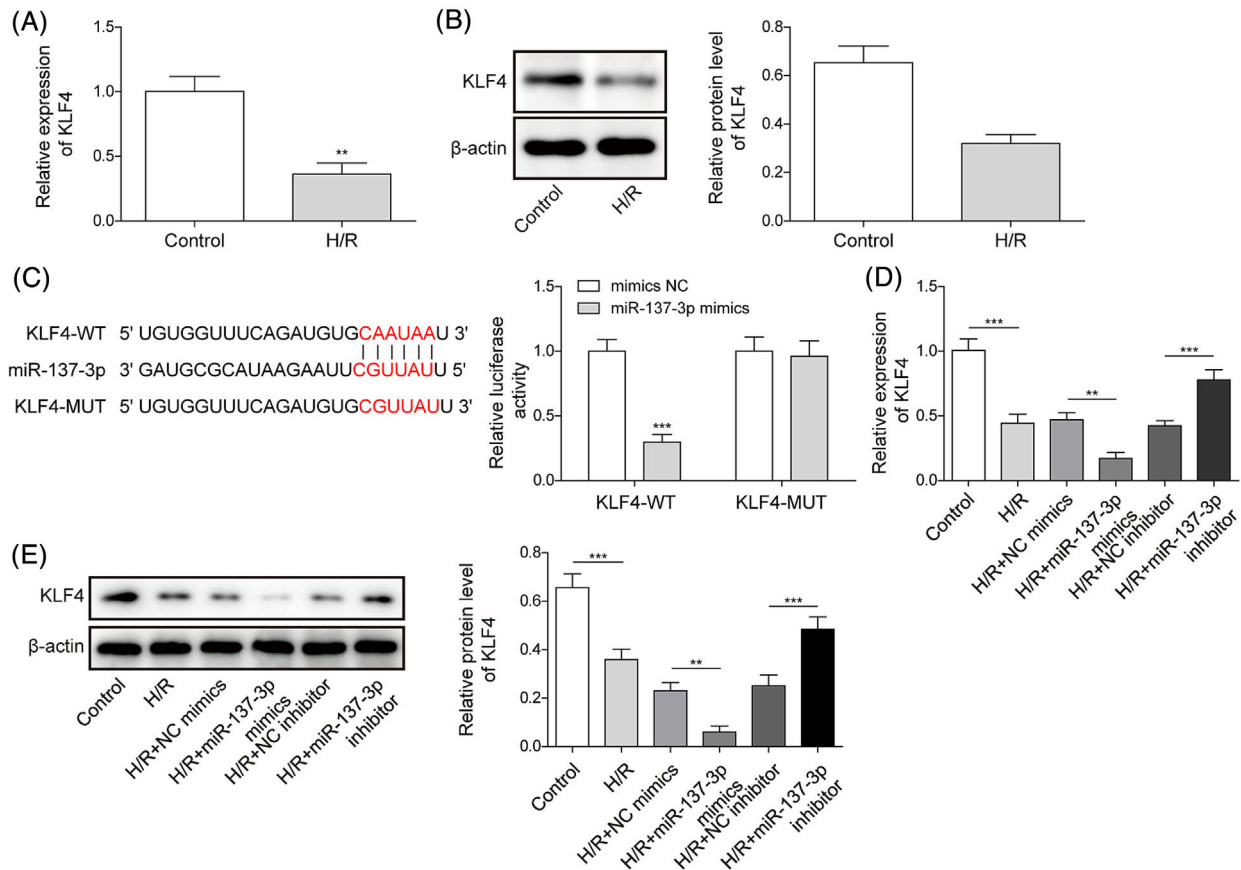
To investigate the interaction between miR-137-3p and KLF4 in regulating pyroptosis in cardiomyocytes during MIRI progression, both miR-137-3p inhibition and KLF4 knockdown were induced in H/R-treated HL-1 cells. In brief, HL-1 cardiomyocytes were transfected with NC inhibitor or miR-137-3p inhibitor and sh-NC or sh-KLF4 for 48 h, followed by hypoxia (16 h)-reoxygenation (6 h). The detailed protocol figure was shown in *Figure 4A*. As shown in *Figure 4B,C*, miR-137-3p inhibitor transfection reduced miR-137-3p expression but increasing KLF4 expression in H/R-treated HL-1 cells, whereas sh-KLF4 transfection reversed the promoting effect of miR-137-3p inhibition on KLF4 expression but had no significant effect on miR-137-3p expression. Functional investigations revealed that miR-137-3p inhibition significantly increased H/R-treated HL-1 cell viability but suppressing H/R-induced

increase in IL-1 $\beta$  and IL-18 secretion levels and pyroptosis, while these changes were eliminated after KLF4 knockdown (*Figure 4D-G*). miR-137-3p inhibition also ameliorated H/R-induced increase in NLRP3, Cleaved caspase 1 and Cleaved Gasdermin-D protein levels in HL-1 cells, while these effects were reversed by KLF4 silencing (*Figure 4H*). Collectively, miR-137-3p silencing alleviated H/R-induced pyroptosis in HL-1 cells by upregulating KLF4.

### KLF4 transcriptionally activated TRPV1 and subsequently activated the AKT pathway in HL-1 cells

TRPV1 acts as a protective role in MIRI.<sup>28</sup> As shown in *Figure 5A*, by using the JASPAR database, KLF4 had potential binding sites to TRPV1 promoter. ChIP assay result subsequently showed that KLF4 directly bound with TRPV1 promoter (*Figure 5B*). Meanwhile, dual luciferase reporter gene assay showed that KLF4 transcriptionally activated TRPV1 (*Figure 5C*). In addition, H/R treatment suppressed the expressions of TRPV1 and p-AKT in HL-1 cells, while KLF4 knockdown further reduced their expressions (*Figure 5D,E*). To sum up, KLF4 activated the AKT pathway by transcriptionally activating TRPV1 in HL-1 cells.

**Figure 3** miR-137-3p inhibited KLF4 expression by directly binding to KLF4. (A, B) HL-1 cells were subjected to H/R treatment, and KLF4 mRNA and protein levels in cells were examined using RT-qPCR and western blot. (C) The potential binding site of between miR-137-3p and KLF4 was presented, and its interaction was affirmed by dual luciferase reporter gene assay. (D, E) KLF4 expression levels in H/R-treated HL-1 cells after miR-137-3p over-expression or miR-137-3p inhibition were examined using RT-qPCR and western blot. The measurement data were presented as mean  $\pm$  SD. All data were obtained from three independent repeated experiments. \* $P < 0.05$ , \*\* $P < 0.01$ , \*\*\* $P < 0.001$ .



### SNHG1 upregulation alleviated H/R-induced pyroptosis in HL-1 cells by regulating the miR-137-3p/KLF4/TRPV1 axis

To illustrate the effects of TRPV1 on lncRNA SNHG1-mediated biological function in MIRI, HL-1 cells were transfected with oe-SNHG1 alone or oe-SNHG1 together with sh-TRPV1, followed by hypoxia (16 h)-reoxygenation (6 h). The detailed protocol figure was shown in *Figure 6A*. It was observed that oe-SNHG1 transfection increased SNHG1 expression and reduced miR-137-3p in H/R-treated HL-1 cells, while TRPV1 knockdown had no significant effect on SNHG1 and miR-137-3p expressions in cells (*Figure 6B*). In addition, SNHG1 overexpression significantly elevated KLF4 and TRPV1 protein levels in H/R-treated HL-1 cells, while the promoting effect of SNHG1 overexpression on TRPV1 protein level was reversed by sh-TRPV1 transfection (*Figure 6C*). SNHG1 overexpression also significantly increased H/R-treated HL-1 cell viability and inhibited H/R-induced increase in IL-1 $\beta$ , IL-18 factor se-

cretion and pyroptosis, while these changes were eliminated after TRPV1 knockdown (*Figure 6D–G*). Meanwhile, H/R-induced increase in NLRP3, Cleaved caspase 1 and Cleaved Gasdermin-D protein levels in HL-1 cells was ameliorated by SNHG1 upregulation, while the changes in the expression of these proteins were eliminated by TRPV1 knockdown (*Figure 6H*). Collectively, TRPV1 knockdown reversed the alleviation of SNHG1 upregulation on H/R-induced pyroptosis in HL-1 cells.

## Discussion

MIRI can cause cardiac arrest and other fatal consequences (known as MIRI), dramatically enhancing the lethality of a myocardial infarction.<sup>29</sup> Pyroptosis is a key player in promoting MIRI progression.<sup>30</sup> Our findings showed that lncRNA SNHG1 alleviated H/R-induced pyroptosis in HL-1 cells by ac-

**Figure 4** miR-137-3p inhibition alleviated H/R-induced pyroptosis in HL-1 cells by increasing KLF4 expression. HL-1 cardiomyocytes were transfected with NC inhibitor or miR-137-3p inhibitor and sh-NC or sh-KLF4 for 48 h, followed by hypoxia (16 h)-reoxygenation (6 h), grouping: Control, H/R, H/R + NC inhibitor, H/R + miR-137-3p inhibitor, H/R + miR-137-3p inhibitor+sh-NC and H/R + miR-137-3p inhibitor+sh-KLF4. (A) The detailed protocol figure was presented. (B) RT-qPCR was performed to detect miR-137-3p and KLF4 expressions in cells. (C) KLF4 protein level in cells was tested by western blot. (D) Cell viability was analysed by MTT assay. (E) ELISA was adopted to detect IL-1 $\beta$  and IL-18 secretion. (F) Cell pyroptosis was analysed using flow cytometry. (G) Cell death was measured by PI staining. (H) Western blot was employed to determine NLRP3, Cleaved caspase 1, and Cleaved Gasdermin-D protein levels in HL-1 cells. The measurement data were presented as mean  $\pm$  SD. All data were obtained from three independent repeated experiments. \* $P < 0.05$ , \*\* $P < 0.01$ , \*\*\* $P < 0.001$ .

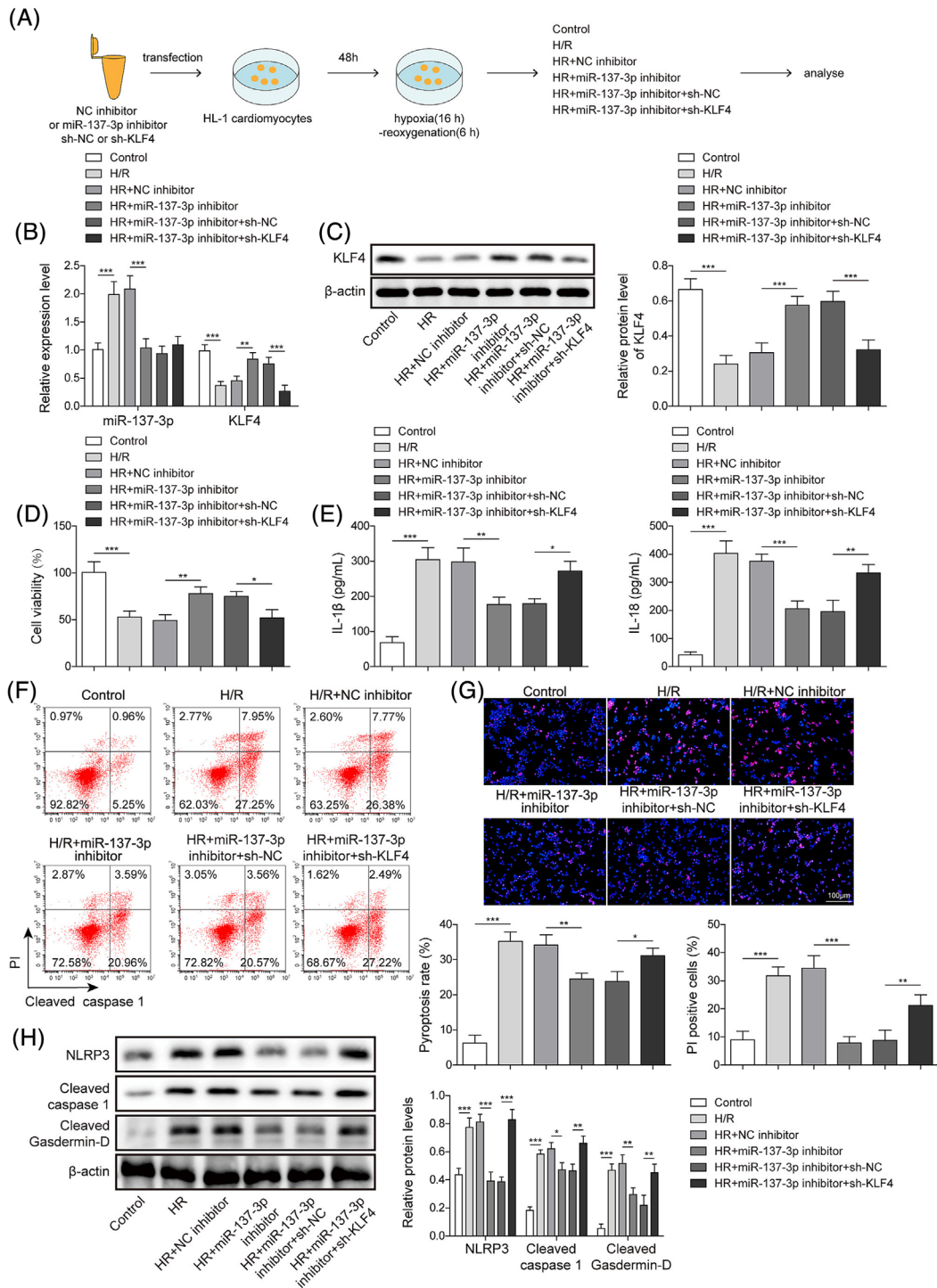
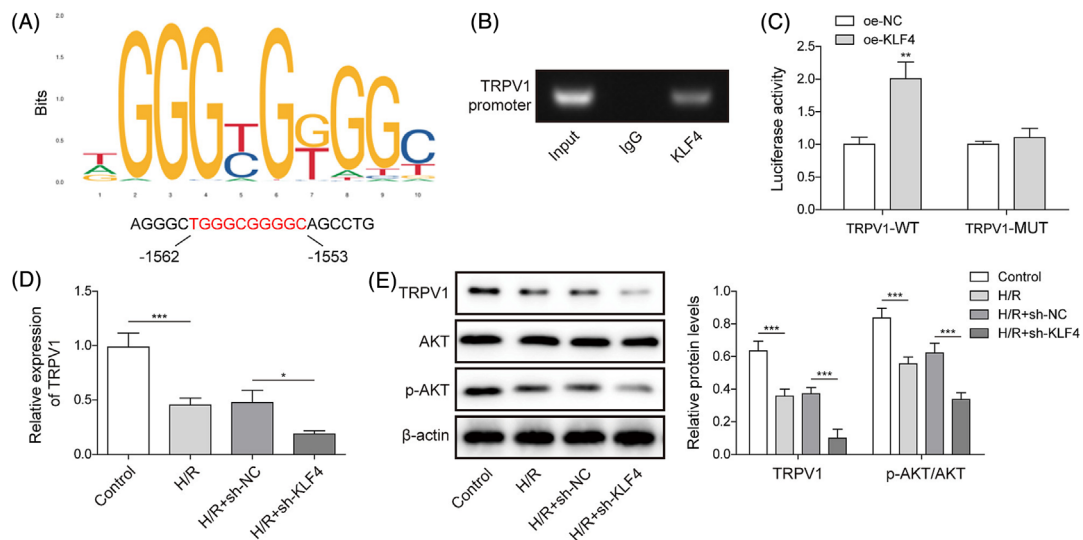




**Figure 5** KLF4 transcriptionally activated TRPV1 and subsequently activated the AKT pathway in HL-1 cells. (A) JASPAR database was employed to predict the potential binding sites between KLF4 and TRPV1 promoter. (B, C) The interaction between KLF4 and TRPV1 promoter was analysed by ChIP and dual luciferase reporter gene assays. H/R-treated HL-1 cells were transfected with sh-NC or sh-KLF4. (D) TRPV1 mRNA level in cells was detected by RT-qPCR. (E) Western blot was employed to determine TRPV1, AKT and p-AKT protein levels in HL-1 cells. The measurement data were presented as mean  $\pm$  SD. All data were obtained from three independent repeated experiments. \* $P < 0.05$ , \*\* $P < 0.01$ , \*\*\* $P < 0.001$ .



tivating the KLF4/TRPV1/AKT axis through sponging miR-137-3p.

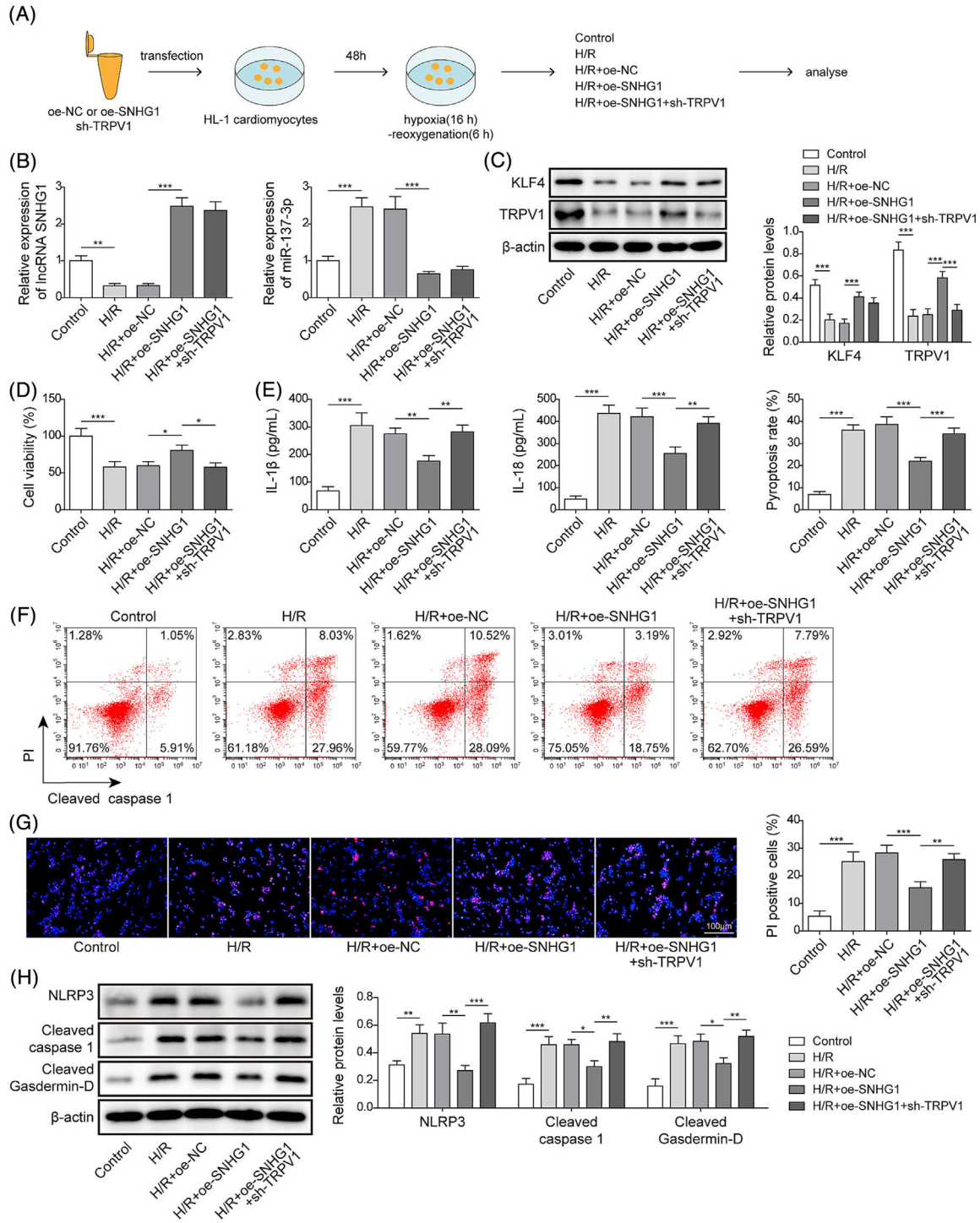
Increasing evidence supports the importance of lncRNAs in MIRI.<sup>31,32</sup> Many studies have shown that lncRNAs can regulate the progression of MIRI by regulating cell viability, apoptosis, and pyroptosis.<sup>33,34</sup> As evidence, lncRNA HCP5 and lncRNA HULC protect against MIRI,<sup>35,36</sup> but lncGAS5 and lncRNA MALAT1 aggravate MIRI.<sup>31,37</sup> In the current study, we confirmed the beneficial effects of lncRNA SNHG1 in H/R-induced HL-1 cells through increasing cell viability, reducing the release of proinflammatory cytokines (IL-1 $\beta$  and IL-18) and suppressing cell pyroptosis. Previous research reported that lncRNA SNHG1 overexpression overtly increased cell viability and arrested apoptosis in H<sub>2</sub>O<sub>2</sub>-treated human cardiomyocytes.<sup>38</sup> Additionally, lncRNA SNHG1 protected human umbilical vein endothelial cell from H/R-induced injury through mediating HIF-1 $\alpha$ /VEGF pathway.<sup>13</sup> Although the functions of lncRNA SNHG1 in MIRI have been studied, the detailed mechanism remains unclear.

In general, lncRNA can interact with miRNA as a competitive endogenous RNA and participate in regulating the expression of target genes.<sup>39</sup> In the current research, we found that lncRNA SNHG1 could engage in H/R-induced HL-1 cell pyroptosis by sponging miR-137-3p. Our results showed that miR-137-3p was highly expressed in H/R-induced HL-1 cells, and its inhibition could alleviate H/R-induced pyroptosis in HL-1 cells. The function of miR-137-3p in MIRI has been studied.<sup>19</sup> For instance, miR-137-3p expression was obviously enhanced in myocardial infarction patients and H/R-treated H9C2 cells, and miR-137-3p inhibition restrained cell apopto-

sis and oxidative stress in H/R-treated H9C2 cells via elevation of KLF15.<sup>19</sup> Our study revealed the role of SNHG1/miR-137-3p in regulating cardiomyocyte pyroptosis during MIRI progression, which has never been reported before.

It is well-known that miRNAs can regulate the expression of target genes at the post-transcriptional level.<sup>16</sup> KLF4 was shown to be a downstream target of miR-137-3p in the current investigation. In addition, KLF4 knockdown reversed the inhibitory effect of miR-137-3p inhibition on H/R-induced cardiomyocyte pyroptosis, which protective effects of KLF4 in MIRI have been confirmed in previous research.<sup>25</sup> Notably, we observed the interaction between KLF4 and TRPV1. As previously depicted, overexpression of TRPV1 inhibited cell apoptosis by activating the PI3K/AKT pathway, thereby assuaging the heart injury by I/R-induced.<sup>22</sup> In addition, Yao et al. demonstrated that oleoylethanolamide (TRPV1 agonist) could reduce myocardial cell apoptosis by activating the PI3K/AKT signalling pathway in diabetic rats with MIRI.<sup>28</sup> Moreover, the allosteric AKT inhibitor (MK-2206) abolished the Aesculin (AES)-mediated cardioprotection and the NLRP3 inflammasome suppression during MIRI development.<sup>40</sup> In this study, it turned out that TRPV1 expression in HL-1 cells was markedly reduced by H/R treatment, and its inhibition could further aggravate H/R-induced cardiomyocytes injury, which could also offset the protective functions of lncRNA SNHG1 sufficiency. As reported, the ischaemia is a combination of lack of oxygen plus nutrients, and some studies applied H/R treatment of the cells combined with nutrient deprivation to mimics MIRI *in vitro*.<sup>6,41</sup> We applied H/R of the cells without nutrient deprivation with reference to some

**Figure 6** SNHG1 upregulation alleviated H/R-induced pyroptosis in HL-1 cells by regulating the miR-137-3p/KLF4/TRPV1 axis. HL-1 cells were transfected with oe-SNHG1 alone or oe-SNHG1 together with sh-TRPV1, followed by hypoxia (16 h)-re-oxygenation (6 h), grouping: Control, H/R, H/R + oe-NC, H/R + oe-SNHG1 and H/R + oe-SNHG1 + sh-TRPV1. (A) The detailed protocol figure was presented. (B) RT-qPCR was performed to detect SNHG1 and miR-137-3p expressions in cells. (C) KLF4 and TRPV1 protein levels in cells were assessed by western blot. (D) Cell viability was analysed by MTT assay. (E) ELISA was adopted to detect IL-1 $\beta$  and IL-18 secretion. (F) Cell pyroptosis was analysed using flow cytometry. (G) Cell death was measured by PI staining. (H) Western blot was employed to determine NLRP3, Cleaved caspase 1, and Cleaved Gasdermin-D protein levels in HL-1 cells. The measurement data were presented as mean  $\pm$  SD. All data were obtained from three independent repeated experiments. \* $P < 0.05$ , \*\* $P < 0.01$ , \*\*\* $P < 0.001$ .



researches.<sup>42,43</sup> HL-1 cardiomyocytes are currently the only cells available that continuously divide, spontaneously contract, and maintain a differentiated adult cardiac phenotype through indefinite passages in culture.<sup>44</sup> HL-1 cells have also been used to address pathological conditions such as hypoxia, hyperglycemia-hyperinsulinemia, apoptosis, and I/R.<sup>45</sup> However, the expression patterns of cardiomyocyte markers and whole transcriptomic profile indicate low-to-moderate similarity of HL-1 cells to primary cells/cardiac tissues.<sup>46</sup> We will validate the role of lncRNA SNHG1/miR0137-3p/KLF4/TRPV1 axis in MIRI using primary myocardial cells in future experiments.

Taken together, our findings show that lncRNA SNHG1 suppresses H/R-induced pyroptosis of cardiomyocytes and upregulates the KLF4/TRPV1 axis by competitively binding to miR-137-3p, presenting a new target for MIRI treatment. However, limitations remain in this study. For example, we only provide experimental data at the cellular level, and neither animal experiments nor clinical samples are involved. To increase the accuracy of the research, further research is necessary at the animal level and downstream signalling pathways in MIRI.

## Acknowledgements

Not applicable.

## Conflict of interest

These authors declared no competing interests in this work.

## References

1. Reed GW, Rossi JE, Cannon CP. Acute myocardial infarction. *Lancet* 2017;**389**: 197–210. doi:10.1016/S0140-6736(16)30677-8
2. Hausenloy DJ, Yellon DM. Myocardial ischemia-reperfusion injury: a neglected therapeutic target. *J Clin Invest* 2013;**123**:92–100. doi:10.1172/JCI62874
3. Bortolotti P, Faure E, Kipnis E. Inflammasomes in tissue damages and immune disorders after trauma. *Front Immunol* 2018;**9**:1900. doi:10.3389/fimmu.2018.01900
4. Frank D, Vince JE. Pyroptosis versus necroptosis: Similarities, differences, and crosstalk. *Cell Death Differ* 2019;**26**:99–114. doi:10.1038/s41418-018-0212-6
5. Toldo S, Mauro AG, Cutter Z, Abbate A. Inflammasome, pyroptosis, and cytokines in myocardial ischemia-reperfusion injury. *Am J Physiol Heart Circ Physiol* 2018;**315**:H1553–h1568. doi:10.1152/ajpheart.00158.2018
6. Zhang J, Huang L, Shi X, Yang L, Hua F, Ma J, et al. Metformin protects against myocardial ischemia-reperfusion injury and cell pyroptosis via AMPK/NLRP3 inflammasome pathway. *Aging (Albany NY)* 2020;**12**:24270–24287. doi:10.18632/aging.202143
7. Ferrè F, Colantoni A, Helmer-Citterich M. Revealing protein-lncRNA interaction. *Brief Bioinform* 2016;**17**:106–116. doi:10.1093/bib/bbv031
8. Yu B, Wang S. Angio-lncRs: lncRNAs that regulate angiogenesis and vascular disease. *Theranostics* 2018;**8**:3654–3675. doi:10.7150/thno.26024
9. Ghafouri-Fard S, Shoorei H, Taheri M. Non-coding RNAs participate in the ischemia-reperfusion injury. *Biomed Pharmacother* 2020;**129**:110419. doi:10.1016/j.biopha.2020.110419
10. Niu X, Pu S, Ling C, Xu J, Wang J, Sun S, et al. lncRNA Oip5-as1 attenuates myocardial ischaemia/reperfusion injury by sponging miR-29a to activate the SIRT1/AMPK/PGC1 $\alpha$  pathway. *Cell Prolif* 2020;**53**:e12818. doi:10.1111/cpr.12818
11. Pei YH, Chen J, Wu X, He Y, Qin W, He SY, et al. lncRNA PEAMIR inhibits apoptosis and inflammatory response in PM2.5 exposure aggravated myocardial ischemia/reperfusion injury as a competing endogenous RNA of miR-29b-3p. *Nanotoxicology* 2020;**14**:638–653. doi:10.1080/17435390.2020.1731857
12. Hu C, Wang S, Liu L. Long non-coding RNA small nucleolar RNA host gene 1 alleviates the progression of epilepsy by regulating the miR-181a/BCL-2 axis in

## Funding

This work was supported by the National Natural Science Foundation of China (No. 81800391) and Science and Technology Innovation Cultivation Foundation of Zhongnan Hospital of Wuhan University (project number: CXPY2020006).

## Supporting information

Additional supporting information may be found online in the Supporting Information section at the end of the article.

**Figure S1.** The diagram of transfection was presented.

**Figure S2.** HL-1 cells were transfected with oe-NC or oe-SNHG1. (A) RT-qPCR was performed to detect SNHG1 expression in cells. (B) Cell viability was analysed by MTT assay. (C) Cell pyroptosis was analysed using flow cytometry. The measurement data were presented as mean  $\pm$  SD. All data were obtained from three independent repeated experiments. \* $P < 0.05$ , \*\* $P < 0.01$ , \*\*\* $P < 0.001$ .

**Figure S3.** HL-1 cells were treated with 5  $\mu$ M metoprolol for 24 h and then exposed to H/R stimulation. HL-1 cell viability was detected by MTT assay. The measurement data were presented as mean  $\pm$  SD. All data were obtained from three independent repeated experiments. \* $P < 0.05$ , \*\* $P < 0.01$ , \*\*\* $P < 0.001$ .

- vitro. *Life Sci* 2021;**267**:118935. doi:10.1016/j.lfs.2020.118935
13. Liang S, Ren K, Li B, Li F, Liang Z, Hu J, et al. LncRNA SNHG1 alleviates hypoxia-reoxygenation-induced vascular endothelial cell injury as a competing endogenous RNA through the HIF-1 $\alpha$ /VEGF signal pathway. *Mol Cell Biochem* 2020;**465**:1-11. doi:10.1007/s11010-019-03662-0
  14. Xu M, Chen X, Lin K, Zeng K, Liu X, Pan B, et al. The long noncoding RNA SNHG1 regulates colorectal cancer cell growth through interactions with EZH2 and miR-154-5p. *Mol Cancer* 2018;**17**:141. doi:10.1186/s12943-018-0894-x
  15. Yan SM, Li H, Shu Q, Wu WJ, Luo XM, Lu L. LncRNA SNHG1 exerts a protective role in cardiomyocytes hypertrophy via targeting miR-15a-5p/HMG1 axis. *Cell Biol Int* 2020;**44**:1009-1019. doi:10.1002/cbin.11298
  16. Bartel DP. MicroRNAs: Target recognition and regulatory functions. *Cell* 2009;**136**:215-233. doi:10.1016/j.cell.2009.01.002
  17. Liu B, Li J, Cairns MJ. Identifying miRNAs, targets and functions. *Brief Bioinform* 2014;**15**:1-19. doi:10.1093/bib/bbs075
  18. Wang JX, Zhang XJ, Li Q, Wang K, Wang Y, Jiao JQ, et al. MicroRNA-103/107 regulate programmed necrosis and myocardial ischemia/reperfusion injury through targeting FADD. *Circ Res* 2015;**117**:352-363. doi:10.1161/CIRCRESA-HA.117.305781
  19. Zhao T, Qiu Z, Gao Y. MiR-137-3p exacerbates the ischemia-reperfusion injured cardiomyocyte apoptosis by targeting KLF15. *Naunyn Schmiedebergs Arch Pharmacol* 2020;**393**:1013-1024. doi:10.1007/s00210-019-01728-w
  20. Wang H, Yu Q, Zhang ZL, Ma H, Li XQ. Involvement of the miR-137-3p/CAPN-2 interaction in ischemia-reperfusion-induced neuronal apoptosis through modulation of p35 cleavage and subsequent Caspase-8 Overactivation. *Oxid Med Cell Longev* 2020;**2020**:2616871. doi:10.1155/2020/2616871
  21. Zang Y, Zhu J, Li Q, Tu J, Li X, Hu R, et al. miR-137-3p modulates the progression of prostate cancer by regulating the JNK3/EZH2 Axis. *Onco Targets Ther* 2020;**13**:7921-7932. doi:10.2147/OTT.S256161
  22. Jiang XX, Liu GY, Lei H, Li ZL, Feng QP, Huang W. Activation of transient receptor potential vanilloid 1 protects the heart against apoptosis in ischemia/reperfusion injury through upregulating the PI3K/Akt signaling pathway. *Int J Mol Med* 2018;**41**:1724-1730. doi:10.3892/ijmm.2017.3338
  23. Randhawa PK, Jaggi AS. A review on potential involvement of TRPV(1) channels in ischemia-reperfusion injury. *J Cardiovasc Pharmacol Ther* 2018;**23**:38-45. doi:10.1177/1074248417707050
  24. Zhong B, Wang DH. Protease-activated receptor 2-mediated protection of myocardial ischemia-reperfusion injury: Role of transient receptor potential vanilloid receptors. *Am J Physiol Regul Integr Comp Physiol* 2009;**297**:R1681-R1690. doi:10.1152/ajpregu.90746.2008
  25. Wu Q, Wang H, He F, Zheng J, Zhang H, Cheng C, et al. Depletion of microRNA-92a enhances the role of sevoflurane treatment in reducing myocardial ischemia-reperfusion injury by upregulating KLF4. *Cardiovasc Drugs Ther* 2022;**37**:1053-1064. doi:10.1007/s10557-021-07303-x
  26. Lv XW, Wang MJ, Qin QY, Lu P, Qin GW. 6-Gingerol relieves myocardial ischaemia/reperfusion injury by regulating lncRNA H19/miR-143/ATG7 signaling axis-mediated autophagy. *Lab Invest* 2021;**101**:865-877. doi:10.1038/s41374-021-00575-9
  27. Kleinbongard P. Cardioprotection by early metoprolol-attenuation of ischemic vs. reperfusion injury? *Basic Res Cardiol* 2020;**115**:54. doi:10.1007/s00395-020-0814-2
  28. Yao E, Luo L, Lin C, Wen J, Li Y, Ren T, et al. OEA alleviates apoptosis in diabetic rats with myocardial ischemia/reperfusion injury by regulating the PI3K/Akt signaling pathway through activation of TRPV1. *Front Pharmacol* 2022;**13**:964475. doi:10.3389/fphar.2022.964475
  29. Shen Y, Liu X, Shi J, Wu X. Involvement of Nrf2 in myocardial ischemia and reperfusion injury. *Int J Biol Macromol* 2019;**125**:496-502. doi:10.1016/j.ijbiomac.2018.11.190
  30. Qiu Z, Lei S, Zhao B, Wu Y, Su W, Liu M, et al. NLRP3 inflammasome activation-mediated pyroptosis aggravates myocardial ischemia/reperfusion injury in diabetic rats. *Oxid Med Cell Longev* 2017;**2017**:9743280. doi:10.1155/2017/9743280
  31. Xu J, Yu D, Bai X, Zhang P. Long non-coding RNA growth arrest specific transcript 5 acting as a sponge of microRNA-188-5p to regulate SMAD family member 2 expression promotes myocardial ischemia-reperfusion injury. *Bioengineered* 2021;**12**:6674-6686. doi:10.1080/21655979.2021.1957524
  32. Zhao Z, Sun W, Guo Z, Liu B, Yu H, Zhang J. Long noncoding RNAs in myocardial ischemia-reperfusion injury. *Oxid Med Cell Longev* 2021;**2021**:8889123. doi:10.1155/2021/2801263
  33. Kang H, Yu H, Zeng L, Ma H, Cao G. LncRNA Rian reduces cardiomyocyte pyroptosis and alleviates myocardial ischemia-reperfusion injury by regulating the miR-17-5p/CCND1 axis. *Hypertens Res* 2022;**45**:976-989. doi:10.1038/s41440-022-00884-6
  34. Yu SY, Dong B, Fang ZF, Hu XQ, Tang L, Zhou SH. Knockdown of lncRNA AK139328 alleviates myocardial ischaemia/reperfusion injury in diabetic mice via modulating miR-204-3p and inhibiting autophagy. *J Cell Mol Med* 2018;**22**:4886-4898. doi:10.1111/jcmm.13754
  35. Li KS, Bai Y, Li J, Li SL, Pan J, Cheng YQ, et al. LncRNA HCP5 in hBMSC-derived exosomes alleviates myocardial ischemia reperfusion injury by sponging miR-497 to activate IGF1/PI3K/AKT pathway. *Int J Cardiol* 2021;**342**:72-81. doi:10.1016/j.ijcard.2021.07.042
  36. Liang H, Li F, Li H, Wang R, du M. Overexpression of lncRNA HULC attenuates myocardial ischemia/reperfusion injury in rat models and apoptosis of hypoxia/reoxygenation cardiomyocytes via targeting miR-377-5p through NLRP3/caspase-1/IL-1 $\beta$  signaling pathway inhibition. *Immunol Invest* 2021;**50**:925-938. doi:10.1080/08820139.2020.1791178
  37. Yin Y, Lu X, Yang M, Shangguan J, Zhang Y. Inhibition of lncRNA MALAT1 reduces myocardial ischemia-reperfusion injury of rat cardiomyocytes through regulating the miR-135a-5p/HIF1AN axis. *J Gene Med* 2021;**e3392**. doi:10.1002/jgm.3392
  38. Zhang N, Meng X, Mei L, Hu J, Zhao C, Chen W. The long non-coding RNA SNHG1 attenuates cell apoptosis by regulating miR-195 and BCL2-like protein 2 in human cardiomyocytes. *Cell Physiol Biochem* 2018;**50**:1029-1040. doi:10.1159/000494514
  39. Huang Y. The novel regulatory role of lncRNA-miRNA-mRNA axis in cardiovascular diseases. *J Cell Mol Med* 2018;**22**:5768-5775. doi:10.1111/jcmm.13866
  40. Xu XN, Jiang Y, Yan LY, Yin SY, Wang YH, Wang SB, et al. Aesculin suppresses the NLRP3 inflammasome-mediated pyroptosis via the Akt/GSK3 $\beta$ /NF- $\kappa$ B pathway to mitigate myocardial ischemia/reperfusion injury. *Phytomedicine* 2021;**92**:153687. doi:10.1016/j.phymed.2021.153687
  41. Makkos A, Szántai Á, Pálóczi J, Pipis J, Kiss B, Poggi P, et al. A comorbidity model of myocardial ischemia/reperfusion injury and hypercholesterolemia in rat cardiac myocyte cultures. *Front Physiol* 2019;**10**:1564. doi:10.3389/fphys.2019.01564
  42. Shen S, He F, Cheng C, Xu BL, Sheng JL. Uric acid aggravates myocardial ischemia-reperfusion injury via ROS/NLRP3 pyroptosis pathway. *Biomed Pharmacother* 2021;**133**:110990. doi:10.1016/j.biopha.2021.110990
  43. Zhang CX, Cheng Y, Liu DZ, Liu M, Cui H, Zhang BL, et al. Mitochondria-targeted cyclosporin A delivery system to treat myocardial ischemia reperfusion injury of rats. *J Nanobiotechnology* 2019;**17**:18. doi:10.1186/s12951-019-0451-9
  44. Claycomb WC, Lanson NA Jr, Stallworth BS, Egeland DB, Delcarpio JB, Bahinski A, et al. HL-1 cells: A cardiac muscle cell line that contracts and retains phenotypic characteristics of the adult cardiomyocyte. *Proc Natl Acad Sci U S A*



- 1998;**95**:2979-2984. doi:[10.1073/pnas.95.6.2979](https://doi.org/10.1073/pnas.95.6.2979)
45. White SM, Constantin PE, Claycomb WC. Cardiac physiology at the cellular level: Use of cultured HL-1 cardiomyocytes for studies of cardiac muscle cell structure and function. *Am J Physiol Heart Circ Physiol* 2004;**286**:H823-H829. doi:[10.1152/ajpheart.00986.2003](https://doi.org/10.1152/ajpheart.00986.2003)
46. Onódi Z, Visnovitz T, Kiss B, Hambalkó S, Koncz A, Ágg B, *et al.* Systematic transcriptomic and phenotypic characterization of human and murine cardiac myocyte cell lines and primary cardiomyocytes reveals serious limitations and low resemblances to adult cardiac phenotype. *J Mol Cell Cardiol* 2022;**165**:19-30. doi:[10.1016/j.yjmcc.2021.12.007](https://doi.org/10.1016/j.yjmcc.2021.12.007)